Tumor Cell Membrane-Encapsulated Polymeric Nanoparticles for Preparation of Biomimetic Cancer Vaccines

Bowen Shen

Shanghai Starriver Bilingual School, Shanghai, China
Email: shenbowen200905@hotmail.com

***Abstract*—Cancer remains one of the most challenging diseases to treat. Recent advances in immunotherapy and cancer vaccines have shown great potential by harnessing the body's immune system to generate durable anti-tumor responses. Despite this progress, effective cancer vaccination still faces major hurdles, particularly in achieving efficient antigen delivery and presentation. In this study, Fluorinated Polyethyleneimine (F-PEI) was synthesized through a ring-opening reaction, in which the amino groups of PEI served as nucleophiles to attack a fluorinated epoxide. This reaction grafted fluorinated alkyl chains onto the polymer backbone, yielding F-PEI with preserved amines and newly introduced hydroxyl groups. To translate this material into a nanovaccine platform, F-PEI nanoparticles were subsequently coated with whole tumor cell membranes (M/F-PEI), thereby integrating the broad antigenic repertoire of the source cell with a chemically engineered nanoparticle core optimized for delivery. Comprehensive characterization confirmed successful membrane coating, producing uniform and stable particles of approximately 200 nm in diameter. Cytotoxicity assays indicated good biocompatibility, with cell viability consistently above 80%. Importantly, the fluorous modification substantially enhanced cellular internalization: uptake by antigen-presenting cells was more than doubled compared with membrane vesicles alone. This increased interaction at the nano–bio interface translated into superior antigen cross-presentation and robust cytokine release, with IL-12 and IL-2 secretion exceeding 1200 pg/mL and 1500 pg/mL, respectively, consistent with strong T-cell activation. Together, these findings highlight the M/F-PEI nanovaccine as a highly promising platform for developing effective cancer immunotherapies.**

***Keywords*—cancer nanovaccine, tumor cell membrane, polyethyleneimine, antigen presentation, dendritic cell, immunotherapy**

I. Introduction

Cancer vaccines have emerged as one of the most promising approaches for achieving precise and long-lasting anti-tumor responses, attracting significant attention in cancer immunotherapy [1]. Analogous to traditional vaccines that train immune cells to recognize and remember pathogen-derived antigens, cancer vaccines are designed to elicit robust tumor-specific immunity. Their primary goal is to enhance antigen-specific T cell activation in patients who otherwise fail to mount sufficient immune responses [2]. By reprogramming the immunosuppressive Tumor Microenvironment (TME), cancer vaccines promote immune cell infiltration and function, enabling recognition of Tumor-Associated Antigens (TAAs) or Tumor-Specific Antigens (TSAs) and ultimately promoting effective anti-tumor immunity [3].

Despite this promise, cancer vaccines still face critical challenges. Tumor cells often display low antigenicity, limiting their recognition by immune cells. Furthermore, cancer immune editing—a unique TME-associated mechanism—allows tumor cells to evade immune surveillance and accelerate metastasis [4]. Overcoming these barriers remains central to the development of effective cancer vaccines.

Cancer vaccines are generally classified into three categories: peptide and protein-based vaccines, cellular vaccines, and genetic vaccines [2]. The peptide vaccine is relatively easy to manufacture, but its benefits are limited because the Human Leukocyte Antigen (HLA) haplotype may not always present the selected antigen. Improvements have been developed by replacing the original short peptide with synthetic long peptides or by using nanoparticles as a delivery platform. However, long peptide synthesis is expensive and inefficient for large-scale production, while nanoparticle platforms have thus far exhibited low antigen presentation efficiency. Cell-based cancer vaccines typically involve the use of DCs loaded with tumor neoantigens, modified autologous cancer cells, and allogeneic tumor cell lines. Although T cell-directed vaccines have shown improved clinical outcomes, their overall therapeutic efficacy in patients remains modest [5]. Genetic vaccines are often virus-based, as virus DNA or RNA may activate DCs by triggering pattern recognition receptors. However, neither the virus-based nor the plasmid vector-based vaccines have yet produced the expected effect, despite extensive research and ongoing optimization [6, 7].

Immunotherapy has attracted considerable attention as an alternative to traditional cancer treatments [8]. Conventional methods such as surgical resection, radiotherapy, and chemotherapy all carry significant limitations. Surgery may damage healthy tissue and does

Manuscript received December 9, 2025; accepted December 29, 2025; published February 6, 2026.

doi: 10.18178/ijpmbs.15.1.1-7

not always remove metastasized tumor cells. Radiotherapy is rarely curative as a standalone treatment [9]. Chemotherapy often impairs the patient's immune system, compromising long-term health [10]. In contrast, immunotherapy offers substantial advantages, including reduced systemic toxicity and the ability to induce long-term immune memory.

Building on these advantages, researchers have increasingly explored the use of nanoparticles to enhance cancer vaccines and other immunotherapies. Current applications of nanoparticles in cancer treatment include targeted delivery systems, mRNA delivery platforms, lymph node–targeted lipid nanoparticles, and tumor antigen delivery [11]. Among these, polymeric nanoparticles are biodegradable and highly modifiable, showing potent antitumor effects by targeting dendritic cells and mitochondria [12]. Aluminum-based nanoparticles are commonly used as vaccine adjuvants to induce strong cell-mediated immunity [13], while virus and virus-like nanoparticles, such as those used in the HPV vaccine, are already licensed for worldwide use.

Despite these advances, the recently used nanoparticles still need refinement before broad clinical application. Key challenges include poor reproducibility in achieving uniform size and morphology, loss of unique properties due to aggregation, rapid systemic clearance, and instability under physiological conditions [14]. Among potential alternatives, Polyethyleneimine (PEI) nanoparticles have attracted considerable attention. PEI chain carries a high density of positive charge, which facilitates the efficient binding with negatively charged biomolecules, including proteins. The physicochemical properties facilitate the accurate modifications and fulfill special needs. However, to date, PEI has not been fully explored as a vaccine delivery platform.Current nanoparticle-based nanovaccines combine the advantages of enhanced antigen delivery and presentation with improved uptake by Antigen-Presenting Cells (APCs) [15, 16]. In addition, it can also remodel the TEM and disrupt the immune escape mechanism. The high permeability and strong retention effect can improve their accumulation in tumor sites. Various types of nanoparticles, including polymeric nanoparticles, liposomes, viruses, and inorganic nanoparticles, have attracted great interest in the vaccine research fields [17, 18].

In this study, we designed a nanovaccine platform based on PEI nanoparticles chemically modified with fluorous ligands to deliver the tumor cell membranes to T-cells to generate the immune response to cancer (Fig. 1). Fluorinated PEI nanoparticles exhibited enhanced affinity for phospholipid bilayers, enabling efficient membrane coating and reducing preparation time. In addition, their nanoscale dimensions approximate those of pathogenic microbes, thereby facilitating uptake by APCs. By covering the whole cell membranes that contain all various TAAs and TSAs, our vaccine manufacturing does not need to identify and design a specific structure targeting these antigens, which are hard to recognize. We modified the fluorescent mark CD11 antibody on the PEI and observed the colored label to determine the uptake and antigen-presenting effect. This approach is beneficial for manufacturing and can contribute to further use in clinical treatment. Additional studies about the vaccine's effect on the living body are needed.

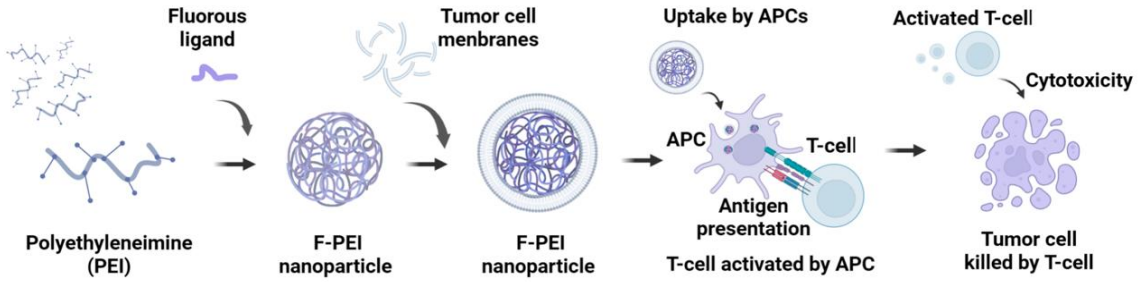

Fig. 1. The schematic illustration of the M/F-PEI mediated cancer immunotherapy.

II. Methods and Materials

A. The Preparation of Membrane-Coated F-PEI Nanoparticle

The reaction mechanism for the synthesis of F-PEI involves a ring-opening reaction between PEI and a fluorinated epoxide (Fig. 2). PEI, with its abundant amino groups ($-NH_2$ and $-NH-$), acts as a nucleophile. The fluorinated epoxide has a strained three-membered ring (epoxide ring), which is highly reactive. At 25°C in methanol over 48 hours, the lone pair electrons on the nitrogen atom of the amino group in PEI attack the electrophilic carbon atom of the epoxide ring. This attack leads to the opening of the epoxide ring. Subsequently, the fluorinated alkyl chain is introduced onto the PEI backbone (F-PEI).

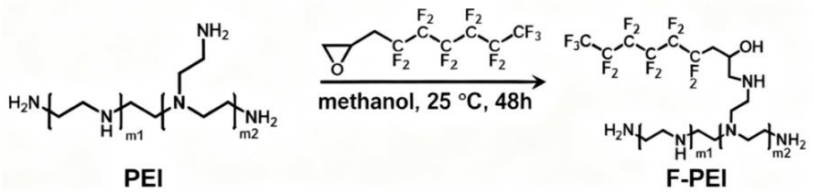

Fig. 2. The synthetic routes of F-PEI.

Specifically, PEI was fluorinated by mixing the PEI solution and the fluorous ligand solution at a molar ratio of 36:1. To a flask, 720 μL of PEI solution and 20 μL of fluorous ligand solution were added. A total of 740 μL of the mixture was stirred thoroughly for 48 hours using a magnetic stirrer until homogeneity was achieved. The obtained F-PEI nanoparticle was dialyzed for 24 hours before 500 μL of tumor cell membranes was added. The membranes and F-PEI were stirred for 2 hours with a magnetic stirrer to form membranes coated with F-PEI nanoparticles (M/F-PEI) (Fig. 3).

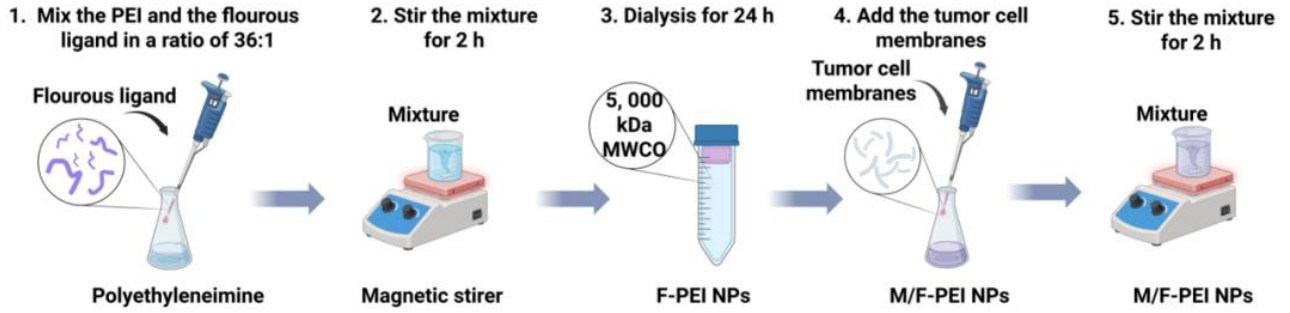

Fig. 3. The illustration of M/F-PEI preparation.

B. Transmission Electron Microscope

The suspension was diluted to the appropriate concentration. A volume of 5 μL of each sample was carefully pipetted and dropped onto copper TEM specimen grids, which were placed on a clean piece of filter paper. The grids were left for 10 minutes at room temperature to allow the nanoparticles to adsorb onto the surface. Excess liquid was wicked away by gently touching the edge of the grid with filter paper. The grid was then transferred to a petri dish and allowed to dry completely for 2 hours. Images of the nanoparticles were taken using a Transmission Electron Microscope (HT7700, Hitachi) after the water had evaporated.

C. CCK-8

Raw264.7 and DC2.4 cells were used as target cells to evaluate the cytotoxicity of M/F-PEI using the CCK-8 assay. The cells were thawed and cultured in a large petri dish containing Dulbecco's Modified Eagle Medium (DMEM) supplemented with 10% Fetal Bovine Serum (FBS) and 1% Penicillin Streptomycin. The medium was replaced when the cells reached 80–90% confluence. The cells were rinsed with 1 mL of PBS, followed by the addition of 1 mL of trypsin to promote detachment. After partial detachment was observed, 2 mL of DMEM was added to neutralize the trypsin. This process was repeated as needed to ensure complete cell detachment. The resulting suspension was centrifuged at 1200 rpm for 3 minutes. The supernatant was carefully removed, and the cell pellet was resuspended in 1 mL of DMEM. A 10 μL aliquot of the resuspended cells was diluted and counted using a hemocytometer to determine the cell density in the 1 mL suspension.

For the CCK-8 assay using 96-well plates, a minimum of 5000 cells per well (in 100 μL volume) was required. The cell suspension was diluted to the appropriate density and added to the central wells of the plate, with different cell types seeded separately. The surrounding wells were filled with 200 μL of PBS to maintain humidity. The plate was incubated for 24 hours to allow cell attachment and growth.

To assess the toxicity of membrane-coated F-PEI nanoparticles, Raw264.7 and DC2.4 cells were exposed to both treated (M/F-PEI) and untreated nanoparticles (F-PEI only or membranes only). The plate was divided into three experimental groups for each cell type: cells co-incubated with M/F-PEI, with membranes only, and with F-PEI only. After the treatment period, 10 μL of WST-8 reagent was added to each well, and the plate was incubated for 2 hours. The absorbance of each well was measured at 450 nm using a Perkin Elmer Victor X4 2030 Multilabel Reader. A blank control was used to define 100% viability. Cell viability was calculated for each well and averaged across replicates.

D. ELISA

50 ng of biotinylated HLA-A*02:01 pHLA monomers were incubated in 50 μL of blocking buffer (PBS containing 0.5% BSA, 2 mM EDTA, and 0.1% sodium azide) to coat streptavidin-coated 96-well plates (R&D Systems, Cp004) at 4°C overnight. The plates were then washed three times with 1X TBST (TBS with 0.05% Tween-20) using a BioTek 405 TS plate washer. Serial dilutions of IgG were applied to the plates and incubated for 1 hour at room temperature, after which the plates were washed again. Subsequently, the plates were incubated with M/F-PEI for 1 hour and washed, and this incubation-wash cycle was repeated three times. Finally, Tetramethylbenzidine (TMB) substrate (BioLegend, 421101) was added to each well. The reaction was terminated by adding 50 μL of 1N sulfuric acid (Thermo Fisher Scientific, SA212-1). Absorbance at 450 nm was measured using a Synergy H1 Multi-Mode Reader (BioTek).

E. Dynamic Light Scattering (DLS)

The concentration of each nanoparticle sample was adjusted using an appropriate filtered solvent to a final volume of 1 mL, ensuring that the concentration fell within the detection limit of the instrument. The size and zeta potential of the nanoparticles were measured using a Malvern Zetasizer Nanoseries (Malvern, USA). The instrument was switched on and allowed to stabilize for 30

minutes prior to measurement to ensure laser thermal stability. The temperature was maintained at 25°C, and each sample was equilibrated for 2 minutes inside the instrument. The sample was transferred into a cuvette, ensuring that no bubbles adhered to the transparent walls. The cap was sealed, and the cuvette was wiped clean with a lint-free tissue before being inserted into the instrument. The scattering angle was set to an optimal position. The sample was then placed into the machine and measured.

F. Flow Cytometry

A volume of 500 μL per well of a Raw264.7 cell suspension at approximately 5×10^4 cells/mL was incubated in a 24-well plate for 24 hours. Six hours prior to flow cytometry analysis, the spent medium was replaced with fresh culture medium. Both media contained 10 μL/mL OVA and 10 μL/mL Chito/OVA/CpG nanoparticles. Each material condition was tested in three replicates. Beckman Coulter nanoparticles were used as a reference standard for the flow cytometry measurements.

The original medium was replaced with 300 μL of PBS, and the Raw264.7 cells were detached by repeated pipetting with PBS. The cell suspension was transferred to flow cytometry test tubes and gently shaken to achieve a homogeneous distribution. The samples were then introduced into the flow cytometer. Live cells and single cells were selected by applying two population gates, and the cells were analyzed based on the AF647 fluorescent signal.

III. Results

A. The Characterization of M-F-PEI NPs

To evaluate the physicochemical properties of the nanoparticles, we employed Transmission Electron Microscopy (TEM) and Dynamic Light Scattering (DLS). TEM images revealed that prior to membrane coating, the nanoparticles lacked any surrounding membrane-like structures (Fig. 4(A)). Following tumor cell membrane coating, however, a distinct transparent, membrane-like layer was clearly observed around the F-PEI nanoparticles (Fig. 4(B)), confirming successful surface modification. DLS analysis was then conducted to determine the hydrodynamic diameter and zeta potential of the membrane-coated nanoparticles. According to Fig. 4(C), the particle size distribution was concentrated in the range of 180–200 nm, a size favorable for uptake by immune cells. The zeta potential measurements indicated a distribution centered around +35 mV (Fig. 4(D)), suggesting good colloidal stability of the M/F-PEI nanoparticles. All the data above is listed in the table (Fig. 4(E)). Altogether, M/F-PEI is easier for immune cells to uptake, thus it is more likely to trigger an immune response against cancer.

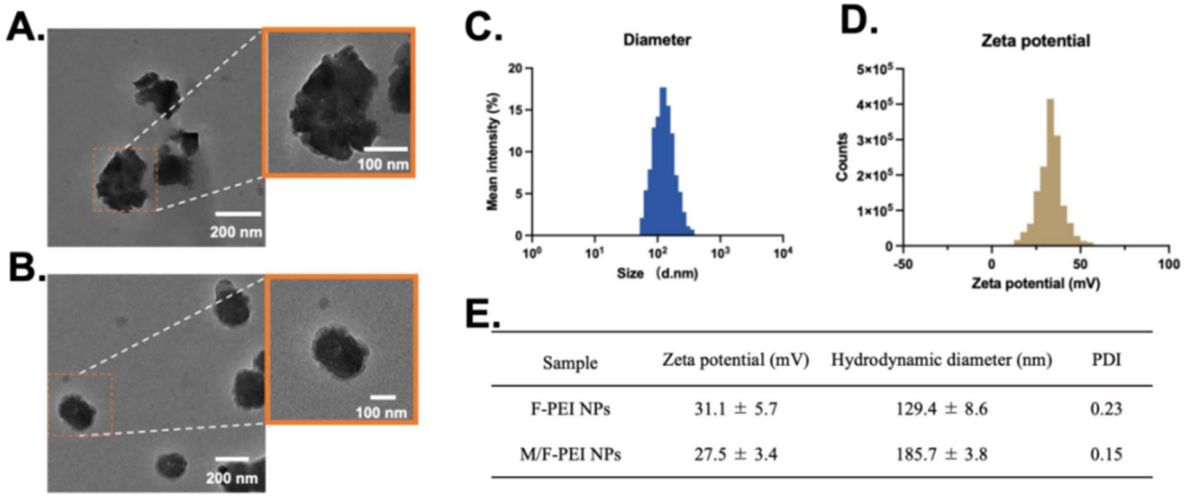

E.

Sample	Zeta potential (mV)	Hydrodynamic diameter (nm)	PDI
F-PEI NPs	31.1 ± 5.7	129.4 ± 8.6	0.23
M/F-PEI NPs	27.5 ± 3.4	185.7 ± 3.8	0.15

Fig. 4. The characterization of M-F-PEI NPs. (A) The TEM photo of F-PEI. (B) The TEM picture of M/F-PEI. (C) The diagram of the M/F-PEI diameter. (D) The diagram of the M/F-PEI zeta potential. (E) The data comparison table of F-PEI and M/F-PEI.

B. The Favorable Biocompatibility of M-F-PEI NPs

To assess the cytotoxicity of the nanoparticles, we performed the CCK-8 experiment n DC2.4 and RAW264.7 cells. According to Fig. 5(A), the cell viability of DC2.4 is about 100% in the absence of nanoparticles and remained above 95% at a concentration of 1 μg/mL. Even at 5 μg/mL, viability decreased by only ~5%, and the lowest observed viability for DC2.4 cells treated with F-PEI was still close to 90%. Similarly, RAW264.7 cells maintained viability above 80% across all tested concentrations of F-PEI (Fig. 5(B)). We next evaluated the cytotoxicity of membrane-coated F-PEI. For DC2.4, viability was ~100% at 0 μg/mL, > 90% at 1 μg/mL, and slightly below 90% at 5 μg/mL. At 10 μg/mL, viability decreased modestly to ~85%. At the highest concentration (20 μg/mL), the relative cell viability of the DC2.4 is still remained above 80%. For the RAW264.7, the lowest relative cell viability is also above 80%. Altogether, the relative cell viability for both main kinds of immune cells remains above 80% with various concentrations of M/F-PEI, which indicates that the cytotoxicity of the nanoparticle is low, thus safe to use in the human body.

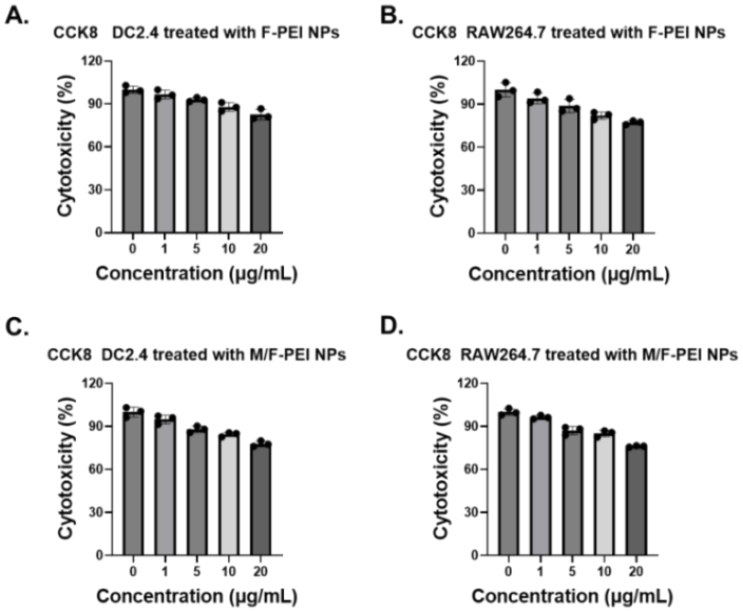

Fig. 5. The cytotoxicity of the F-PEI and the M/F-PEI nanoparticles. (A) The CCK-8 result of DC2.4 treated with F-PEI NPs. (B) The CCK-8 result of RAW264.7 treated with F-PEI NPs. (C) The CCK-8 result of DC2.4 treated with M/F-PEI NPs. (D) The CCK-8 result of RAW264.7 treated with M/F-PEI NPs.

C. The Effective Uptake by Antigen-Presenting Cells

To evaluate whether the M/F-PEI can facilitate the effective uptake of antigen-presenting cells, we conducted Flow cytometry for four samples labeled with AF488, which were blank control, F-PEI NPs, tumor cell membranes only, and M/F-PEI NPs. According to Fig. 6(A), the fluorescence of the blank and F-PEI sample is minimal (3.4% and 4.1%), while the Membranes sample showed a moderate uptake rate of 32.6%. The histogram of M/F-PEI nanoparticles showed that the cellular uptake is significantly stronger than the membranes alone, which indicated that the M/F-PEI can enhance the ability of the immune cells to uptake the nano-vaccines, and then potentially trigger a stronger immune response.

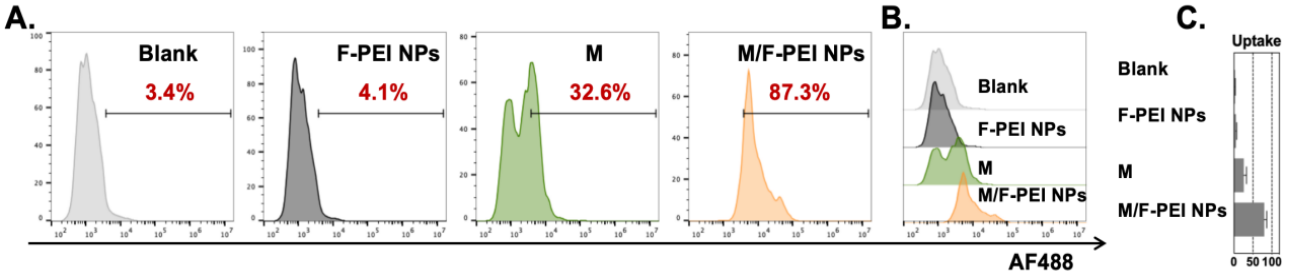

Fig. 6. The effective uptake by antigen-presenting cells. (A) The flow cytometry result analysis of blank, F-PE NPs, Membranes, and M/F-PEI NPs samples. (B) The overlay of the histogram. (C) The statistical result of the flow cytometry data.

D. Cross-Presentation Elicited by M-F-PEI NPs

To investigate the cross-presentation efficiency of the M/F-PEI, dendritic cells were treated with blank control, membrane-only, or M/F-PEI samples and analyzed by flow cytometry. According to Fig. 7(A), 73.9% of cells present the CD11c marker, confirming successful differentiation of bone marrow cells into dendritic cells. Antigen presentation analysis revealed that 88.1% of cells displayed the $OVA_{257–264}$ antigen in the M/F-PEI group, compared with only 3.6% in the membrane-only group (Figs. 7(B) and 7(C)). Altogether, the result shows that using the M/F-PEI to deliver membranes can significantly increase the antigen presentation, potentially triggering a stronger immune response.

E. High Cytokine Levels Secreted by DCs

To determine whether uptake of M/F-PEI nanoparticles promotes cytokine secretion by immune cells, we measured IL-12 and IL-2 levels using ELISA. According to Fig. 8(A), the IL-12 concentration after the cellular uptake of the M/F-PEI is significantly higher than that of the F-PEI, which reaches 1200 pg/mL. The concentration also increases much faster than that of the untreated nanoparticles, which hasn't reached 300 pg/mL at the endpoint. According to Fig. 8(B), the IL-2 concentration also significantly increases and reaches 1700 pg/mL. Altogether, the diagram suggests that both cytokine levels are much higher after using the M/F-PEI nanoparticles to deliver the membranes, which indicates that the DCs are fully activated after the uptake.

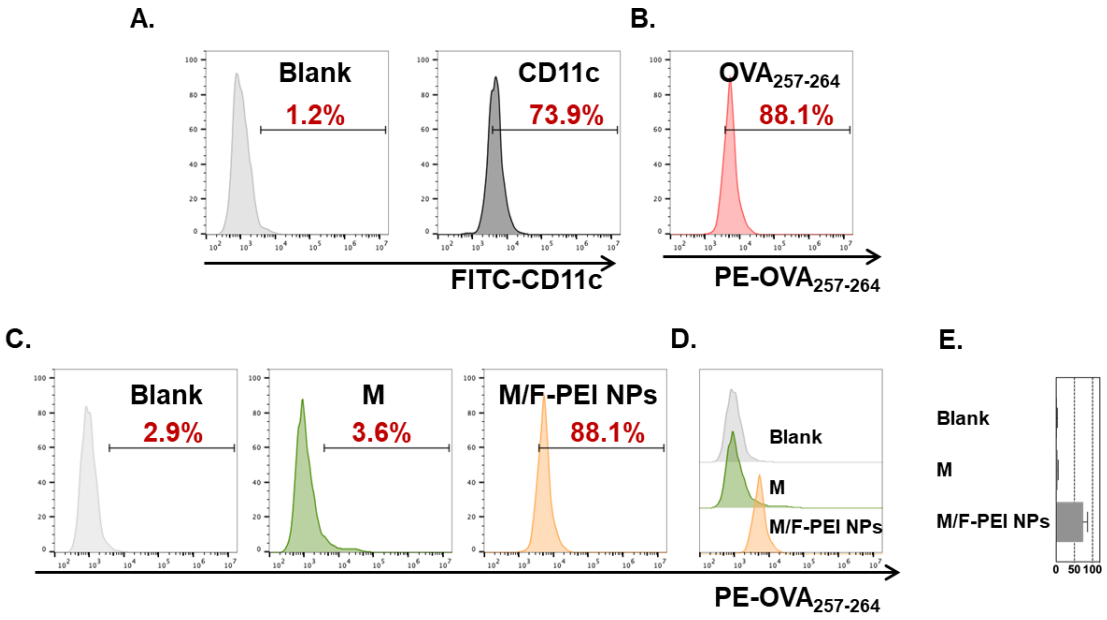

Fig. 7. The data of cross-presentation elicited by M-F-PEI NPs. (A) The representative histogram of flow cytometry analysis of FITC-CD11c presentation. (B) The representative histogram PE-$OVA_{257–264}$ presentation using flow cytometry. (C) The representative histogram analysis of the PE-$OVA_{257–264}$ presentation. (D) The overlay of the histogram of $OVA_{257–624}$ presentation. (E) The statistical result of the cross-presentation efficiency.

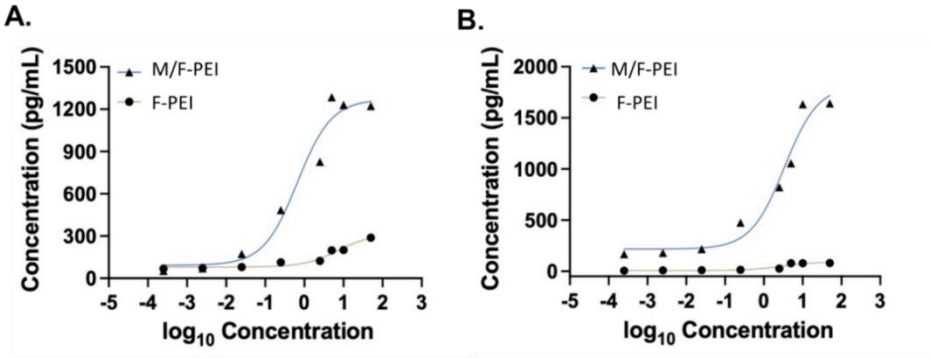

Fig. 8. High cytokine levels secreted by DCs. (A) The diagram of the cytokine-secreting level of IL-12. (B) The diagram of the cytokine-secreting level of IL-2.

IV. Discussion

In this study, we successfully designed and evaluated a novel nanovaccine platform, M/F-PEI, which effectively addresses several key limitations in current cancer vaccine development. By coating fluorous-modified PEI nanoparticles with whole tumor cell membranes, we created a biomimetic particle that combines the advantages of a nanocarrier with the broad antigenic profile of a source tumor cell.

The successful synthesis of fluorous-modified polyethyleneimine nanoparticles (F-PEI) through a ring-opening reaction represents a significant advancement in our study. Fluorination not only improved interactions with cell membranes but also introduced fluorinated alkyl groups that conferred unique properties such as enhanced hydrophobicity and potential targeting ability, which could be beneficial for its application in the development of the biomimetic nanovaccine (M/F-PEI). Our results confirm the successful fabrication of the vaccine. TEM imaging visually confirmed the core-shell structure of M/F-PEI, and DLS data indicated that the resulting nanoparticles were within the ideal size range (~180–200 nm) for efficient uptake by antigen-presenting cells such as dendritic cells [19–21]. The positive zeta potential (~35 mV) contributes to colloidal stability and may also facilitate interaction with the negatively charged cell membranes of APCs, enhancing uptake.

A critical requirement for any clinical translation is biocompatibility [22, 23]. Our CCK-8 assays demonstrated that both the core F-PEI nanoparticles and the final M/F-PEI construct exhibited low cytotoxicity towards immune cells (DC2.4 and RAW264.7), with viability consistently above 80% across a wide concentration range. This suggests a favorable safety profile for in vivo application.

The most significant finding of this work is the dramatic enhancement of immune cell activation. Flow cytometry analysis revealed that the M/F-PEI nanoparticles were taken up by APCs at a significantly higher rate than free tumor cell membranes. This can be attributed to the nano-size and surface properties of the PEI core, which mimics

pathogens and is more readily internalized than micron-sized cellular debris. More importantly, this enhanced uptake translated into superior biological function. Dendritic cells that ingested M/F-PEI nanoparticles exhibited markedly improved cross-presentation, a crucial process for activating cancer-killing CD8+ T-cells [24]. The presentation of the model antigen $OVA_{257–264}$ surged from 3.6% (membranes alone) to 88.1% (M/F-PEI), highlighting the critical role of the nanoparticle platform in processing and presenting encapsulated antigens.

The functional consequences of this enhanced cross-presentation were confirmed by cytokine assays. ELISA revealed a substantial secretion of key T-cell polarizing cytokines, IL-12, and IL-2. This Th1-skewed immune response is essential for activating cytotoxic T lymphocytes and generating a potent, cell-mediated anti-tumor immunity, moving beyond mere antibody responses [2].

Our platform offers a distinct advantage over other vaccine strategies. Unlike peptide vaccines, which are limited by HLA restriction, our approach presents a full spectrum of TAAs and TSAs, making it potentially applicable across a broader patient population without the need for personalized neoantigen identification. Compared to genetic vaccines, which can face delivery and safety hurdles [6], our system uses a stable, synthetic nanoparticle to deliver pre-formed antigens directly to APCs.

In conclusion, the M/F-PEI nanovaccine represents a robust and versatile strategy for cancer immunotherapy. It effectively delivers a broad antigenic payload, enhances APC uptake and cross-presentation, and stimulates a potent Th1-biased cytokine response, all while maintaining excellent biocompatibility. Future work will focus on validating these promising in vitro results in vivo, using animal tumor models to assess the vaccine's efficacy in inhibiting tumor growth, preventing metastasis, and establishing long-term immune memory. This platform holds significant potential for developing a new class of "off-the-shlf" cancer vaccines.

Conflict of Interest

The author declares no conflict of interest.

References

[1] N. Liu, X. Xiao, Z. Zhang, *et al.*, "Advances in cancer vaccine research," *ACS Biomater. Sci. Eng.*, vol. 9, no. 11, pp. 5999–6023, 2023. https://doi.org/10.1021/acsbiomaterials.3c01154

[2] M. A. Morse, W. R. Gwin, and D. A. Mitchell, "Vaccine therapies for cancer: Then and now," *Target Oncol.*, vol. 16, no. 2, pp. 121–152, 2021. https://doi.org/10.1007/s11523-020-00788-w

[3] S. Naskar, N. Sriraman, A. Sarkar, N. Mahajan, and K. Sarkar, "Tumor antigen presentation and the associated signal transduction during carcinogenesis," *Pathol. Res. Pract.*, vol. 261, 155485, 2024. https://doi.org/10.1016/j.prp.2024.155485

[4] Y. Xiao and D. Yu, "Tumor microenvironment as a therapeutic target in cancer," *Pharmacol. Ther.*, vol. 221, 107753, 2021. https://doi.org/10.1016/j.pharmthera.2020.107753

[5] A. D. Waldman, J. M. Fritz, and M. J. Lenardo, "A guide to cancer immunotherapy: From T cell basic science to clinical practice," *Nat. Rev. Immunol.*, vol. 20, no. 11, pp. 651–668, 2020. https://doi.org/10.1038/s41577-020-0306-5

[6] F. Ruzzi, M. S. Semprini, L. Scalambra, *et al.*, "Virus-Like Particle (VLP) vaccines for cancer immunotherapy," *Int. J. Mol. Sci.*, vol. 24, no. 16, 2023. https://doi.org/10.3390/ijms241612963

[7] L. Xie and Y. Li, "Advances in vaccinia virus-based vaccine vectors, with applications in flavivirus vaccine development," *Vaccine*, vol. 40, no. 49, pp. 7022–7031, 2022. https://doi.org/10.1016/j.vaccine.2022.10.047

[8] R. Rui, L. Zhou, and S. He, "Cancer immunotherapies: Advances and bottlenecks," *Front. Immunol.*, vol. 14, 1212476, 2023. https://doi.org/10.3389/fimmu.2023.1212476

[9] S. K. Vinod and E. Hau, "Radiotherapy treatment for lung cancer: Current status and future directions," *Respirology*, vol. 25, suppl. 2, pp. 61–71, 2020. https://doi.org/10.1111/resp.13870

[10] J. Dai, B. Zhang, Y. Su, *et al.*, "Induction chemotherapy followed by radiotherapy vs chemoradiotherapy in nasopharyngeal carcinoma: A randomized clinical trial," *JAMA Oncol.*, vol. 10, no. 4, pp. 456–463, 2024. https://doi.org/10.1001/jamaoncol.2023.6552

[11] L. Miao, Y. Zhang, and L. Huang, "mRNA vaccine for cancer immunotherapy," *Mol. Cancer*, vol. 20, no. 1, p. 41, 2021. https://doi.org/10.1186/s12943-021-01335-5

[12] M. A. Beach, U. Nayanathara, Y. Gao, *et al.*, "Polymeric nanoparticles for drug delivery," *Chem. Rev.*, vol. 124, no. 9, pp. 5505–5616, 2024. https://doi.org/10.1021/acs.chemrev.3c00705

[13] J. Xing, X. Zhao, X. Li, *et al.*, "The recent advances in vaccine adjuvants," *Front. Immunol.*, vol. 16, 1557415, 2025. https://doi.org/10.3389/fimmu.2025.1557415

[14] Q. Lu, D. Kou, S. Lou, *et al.*, "Nanoparticles in tumor microenvironment remodeling and cancer immunotherapy," *J. Hematol. Oncol.*, vol. 17, no. 1, p. 16, 2024. https://doi.org/10.1186/s13045-024-01535-8

[15] S. Chung, C. M. Lee, and M. Zhang, "Advances in nanoparticle-based mRNA delivery for liver cancer and liver-associated infectious diseases," *Nanoscale Horiz.*, vol. 8, no. 1, pp. 10–28, 2022. https://doi.org/10.1039/d2nh00289b

[16] L. Sun, H. Liu, Y. Ye, *et al.*, "Smart nanoparticles for cancer therapy," *Signal Transduct. Target Ther.*, vol. 8, no. 1, 418, 2023. https://doi.org/10.1038/s41392-023-01642-x

[17] N. Fattahi, L. Gorgannezhad, S. F. Masoule, *et al.*, "PEI-based functional materials: Fabrication techniques, properties, and biomedical applications," *Adv. Colloid. Interface Sci.*, vol. 325, 103119, 2024. https://doi.org/10.1016/j.cis.2024.103119

[18] N. Sharma, K. Bietar, and U. Stochaj, "Targeting nanoparticles to malignant tumors," *Biochim. Biophys. Acta Rev. Cancer*, vol. 1877, no. 3, 188703, 2022. https://doi.org/10.1016/j.bbcan.2022.188703

[19] J. A. Champion and S Mitragotri, "Role of target geometry in phagocytosis," *Proc. Natl. Acad. Sci. USA*, vol. 103, no. 13, pp. 4930–4934, 2006. https://doi.org/10.1073/pnas.0600997103

[20] S. E. Gratton, P. A. Ropp, P. D. Pohlhaus, *et al.*, "The effect of particle design on cellular internalization pathways," *Proc. Natl. Acad. Sci. USA*, vol. 105, no. 33, pp. 11613–11618, 2008. https://doi.org/10.1073/pnas.0801763105

[21] C. D. Walkey and W. C. Chan, "Understanding and controlling the interaction of nanomaterials with proteins in a physiological environment," *Chem. Soc. Rev.*, vol. 41, no. 7, pp. 2780–2799, 2012. https://doi.org/10.1039/c1cs15233e

[22] C. Li, L. Chen, D. J. McClements, *et al.*, "Encapsulation of polyphenols in protein-based nanoparticles: Preparation, properties, and applications," *Crit. Rev. Food Sci. Nutr.*, vol. 64, no. 31, pp. 11341–11355, 2024. https://doi.org/10.1080/10408398.2023.2237126

[23] S. Luo, Y. Fu, J. Ye, and C. Liu, "Encapsulation of rutin in protein nanoparticles by pH-driven method: Impact of rutin solubility and mechanisms," *J. Sci. Food Agric.*, vol. 104, no. 3, pp. 1804–1812, 2024. https://doi.org/10.1002/jsfa.13068

[24] Y. Zhou and S. Jiang, "Roles of FcRn in antigen-presenting cells during autoimmunity and a clinical evaluation of efgartigimod as an FcRn blocker," *Pathogens*, vol. 12, no. 6, 2023. https://doi.org/10.3390/pathogens12060817